

Nonlinear feedback coupling in Hindmarsh–Rose neurons

Sunsu Kurian Thottil  · Rose P. Ignatius

Received: 12 May 2016 / Accepted: 18 October 2016 / Published online: 2 November 2016
© Springer Science+Business Media Dordrecht 2016

Abstract We analyse the model of neurons described by Hindmarsh–Rose (H–R) system with various coupling schemes. We have examined the scope of synchronization, anti-phase synchronization and amplitude death for linear indirect synaptic coupling of the H–R neurons. The work is extended to coupling of the form nonlinear cubic feedback. The coupling between two neurons using memristor is also examined. A memristor is now identified as the fourth fundamental circuit element which can be considered as an electrical synapse. Mutual coupling of H–R systems using cubic flux-controlled memristor exhibits the properties of bursting and amplitude death. With unidirectional coupling one neuron exhibits tonic spiking or bursting while the other neuron shows amplitude death. Mutual coupling with quadratic flux-controlled memristor model shows the possibilities of synchronization, oscillation death and other interesting dynamics like near-death rare spikes. Exponential flux-controlled memristor coupling in H–R neuron presents synchronization and oscillation death. We have examined the stability of different coupled systems and the Lyapunov exponent plots. It is shown that among different memristor couplings in H–R neurons, cubic flux-controlled memristor has got highest Lyapunov exponent. The

present work summarizes the simulation results of different coupling schemes in H–R neurons which show many interesting dynamical characteristics of coupled neuron cells.

Keywords Chaos · Amplitude death · Oscillation death · Indirect synaptic coupling · Nonlinear feedback · Memristor coupling · Stability analysis · Lyapunov exponent

1 Introduction

Coupling between same variables of two or more nonlinear systems may lead to synchronization. This has been observed in many physical [1], chemical [2], ecological [3] and biological systems [4]. This phenomenon has found many applications in cryptography and secure communication. Also recent works have shown that coupling nonlinear elements can invoke interesting phenomena, such as hysteresis, phase locking, phase shifting, phase flip, amplitude death [5] and oscillation death [6]. Studies show that synchronization is desirable in cases of quantum devices such as a laser, collective radiation of electrons, in behaviour of insects, and in numerous other instances such as Josephson junction arrays and coupled spin torque nano-oscillators.

Neural synchrony is believed to be an important mechanism underlying many phenomena in the human brain, including the formation of neuronal assemblies

S. K. Thottil (✉) · R. P. Ignatius
Department of Physics, St. Teresa's college, Ernakulam,
Kerala, India
e-mail: sunsukurian@gmail.com

R. P. Ignatius
e-mail: rosgeo@yahoo.com

[7]. In the brain, synchronization is often associated with epileptic form of behaviour [8]. Recent studies [9] show that when an indirect feedback coupling through an environment or an external system is applied to neurons there is a tendency for anti-synchronization, amplitude death and in-phase and out-of-phase synchronization [10]. Also the study of synchronization of synaptically coupled nonlinear oscillators [11] and chimera and study of spatio-temporal dynamics of biological systems [12] are important.

The nonlinear dynamics of a neuron can generate deterministic chaos under some conditions [13]. The coupling schemes for different neurons such as dynamical coupling, time-delay feedback coupling, conjugate coupling, diffusive coupling [14], nonlinear coupling [15], memristor coupling [16], repulsive mean field interaction and damping effect by an environment [9] can be applied to study amplitude death, oscillation death and various other dynamical evolutions of neuron systems.

Oscillation quenching in the form of amplitude death (AD) and oscillation death (OD) is known to appear in oscillatory systems under different coupling schemes. This emergent behaviour in coupled oscillators occurs when they drive each other to a stable equilibrium. In the case of AD, all the coupled oscillators are stabilized to one equilibrium state which may be the origin or any other fixed point. But the coupled systems are stabilized to multiple equilibrium states in the case of OD. This strange phenomenon was, at first, explained as an effect of large parameter mismatch [17] on coupled oscillatory systems. Later, AD was also observed in two identical oscillators when a critical propagation delay [18] is introduced in the coupling. Recent studies [19] unify the mechanism of quenching of oscillation in coupled oscillators, either by a large parameter mismatch or by a delay coupling, or by a common lag scenario. There is numerical as well as experimental evidence for the unknown kind of lag scenario (the lag increases with coupling, and at a critically large value of coupling strength, amplitude death emerges in two largely mismatched oscillators). Coupling schemes such as conjugate type, environment coupling [9] and repulsive feedback link [20] also are found to show the effect of oscillation quenching.

Recent studies of Wang et al. [21] shows the mixed synchronization of H–R neurons under adaptive synchronization. They have found the distribution of syn-

chronization and non-synchronization regions in the two-parameter phase space based on Lyapunov stability theory. Electric activities and signal transmissions among neurons are modulated by autapse. Nowadays study of functional role of autapse on the dynamics of neuronal activities is also an interesting research area. The autapse can induce synchronization, and it will regulate the collective behaviour of neuronal network like a central pacemaker so that all neurons can be regulated to oscillate under identical rhythm [22]. Dynamics of electrical activities in a neuron [23], study of pattern selection and control in neural networks and effect of noise are well discussed by Ma and Tang [24]. They also study effect of electromagnetic radiation on H–R neurons, by introducing an additive variable magnetic flux to original neuron model. Also by imposing time-delayed feedback current in membrane of H–R neuron, its electrical activities are regulated and thus pattern selection in neuronal network is made possible [25].

Synchronization of two nonlinear oscillator systems when coupled through a memristor-like nanoscale device is also an interesting research area [26]. Recently, its applications on neuromorphic computing, device modelling, signal processing, etc., are reported. It is possible to emulate short-term synaptic dynamics with memristive devices where memristor has full potential for building biophysically realistic neural processing systems [27]. When memristor functions as a novel neuro-fuzzy computing system [28], it can be used for creating artificial brain. The mechanism underlying the emergence of synchronization between two memristor coupled Hindmarsh–Rose oscillatory neural cells is also interest of study.

In nervous systems neuron encoding, transferring and integrating information are realized by a series of action potentials [29]. The theoretical and experimental studies on chaotic neural dynamics help to understand higher functions of brain such as adaptation, perception, episodic memory, learning, awareness, intentionality and thought [13]. The studies of dynamical behaviour of neurons are relevant in this context.

Neurons communicate by generating action potentials (potential difference through their cell membranes), which propagate along the axon towards the synapses of other cells. There exist various models, based on systems of ordinary differential equations, which describe the dynamics of action-potential generation for neurons. The equations given by Hodgkin

and Huxley [30], Fitzhugh [31], Morris and Lecar [32] and Hindmarsh and Rose [33] are some of the examples for it. The behaviour of neurons when nonlinear oscillators are coupled together depends on the detailed nature and the strength of the coupling.

In this paper, we wish to address how chaos is employed by neural systems to accomplish biologically important goals such as synchronization, anti-synchronization and oscillation quenching mechanisms for neurons. An appropriate rate equation of neuron model, the Hindmarsh–Rose system is selected to which different coupling schemes are applied. This model equation describes actually a nonlinear dynamical system which demonstrates the pulse propagation in neurons, and is very important from biophysical perspectives [11]. Here the coupling strength summarizes information distribution between neurons. Linear coupling, nonlinear feedback coupling and different memristor-based couplings are applied to the H–R neuron systems to study its dynamics.

In this work it is shown that linear coupling, nonlinear feedback coupling and memristor-based coupling establish a pathway to amplitude death and oscillation death. Amplitude response, amplitude death and phase resetting are analysed in the present work which is having much importance in the study of brain cells. Our work shows possibilities of anti-phase synchronization with linear synaptic coupling, nonlinear cubic feedback coupling, and for unidirectional cubic flux-controlled memristor coupling. The exponential flux-controlled memristor coupling shows many interesting dynamics like near-death rare spikes. Near-death experiences (NDEs) are found to occur as a result of neurobiological alterations in the brain. Cognitive, emotional and transcendental elements comprise NDEs [34].

The study of stability is always a central task for nonlinear differential systems. Here the linear stability analysis [9] for the dynamics of H–R neurons for nonlinear feedback, cubic flux-controlled memristor, quadratic flux-controlled memristor and exponential flux-controlled memristor is performed. The values of Lyapunov exponent (LE) are also computed for the proposed couplings. The neural systems certainly involve nonlinear mechanisms, so the unpredictable and complex behaviour of neural systems can be measured by computation of Lyapunov exponents. If physiological signals have at least one positive Lyapunov exponent, they reflect an unstable and unpre-

dictable system and are used to define deterministic chaos [35]. The largest LE value close to 1 indicates chaotic behaviour. From our plots it is clear that among memristor couplings H–R neurons coupled with cubic flux-controlled memristor exhibits more chaotic nature. In neural systems this value falls due to relaxed situations in the brain [35]. This suggests that when subjects are exposed to external sound or reflexologic stimuli, the brain goes into more relaxed state.

2 Linear coupling in H–R neurons

2.1 Indirect synaptic coupled H–R neurons

Hindmarsh–Rose system model of neurons is described by the equations, which are subjected to linear synaptic and indirect coupled equations. Here we take two neurons with excitatory synaptic coupling and an indirect coupling is introduced between them [9].

$$\begin{aligned}
 \dot{x}_1 &= x_2 - ax_1^3 + bx_1^2 + I_{\text{ext}} - x_3 + \varepsilon u \\
 &\quad + \omega_2 \frac{V_r - x_1}{1 + \exp(-\lambda(x_4 - \theta))} \\
 \dot{x}_2 &= c - dx_1^2 + x_2 \\
 \dot{x}_3 &= r(s(x_1 - x_0) - x_3) \\
 \dot{x}_4 &= x_5 - ax_4^3 + bx_4^2 + I_{\text{ext}} - x_6 + \varepsilon u \\
 &\quad + \omega_2 \frac{V_r - x_4}{1 + \exp(-\lambda(x_1 - \theta))} \\
 \dot{x}_5 &= c - dx_4^2 + x_5 \\
 \dot{x}_6 &= r(s(x_4 - x_0) - x_6) \\
 \dot{u} &= -ku - \frac{\varepsilon}{2} \sum_{i=1,4} x_i
 \end{aligned} \tag{1}$$

The variable x_1 represents the membrane potential of a neuron, and the variables x_2 and x_3 are related ion currents across the membrane. V_r represent the action potential. Here parameters are chosen as $a = 1, b = 3, d = 5, c = 1, I_{\text{ext}} = 3.05, k = 1.6, r = 0.006, s = 4$. The parameters of the system are chosen such that the individual neurons are in the bursting state. Here the synaptic coupling is given by the term $\omega_2 \frac{V_r - x_1}{1 + \exp(-\lambda(x_4 - \theta))}$ and indirect coupling is achieved by an environment through the term u . The last equation which governs the dynamics of u represents the active feedback from both the systems through the environment [9].

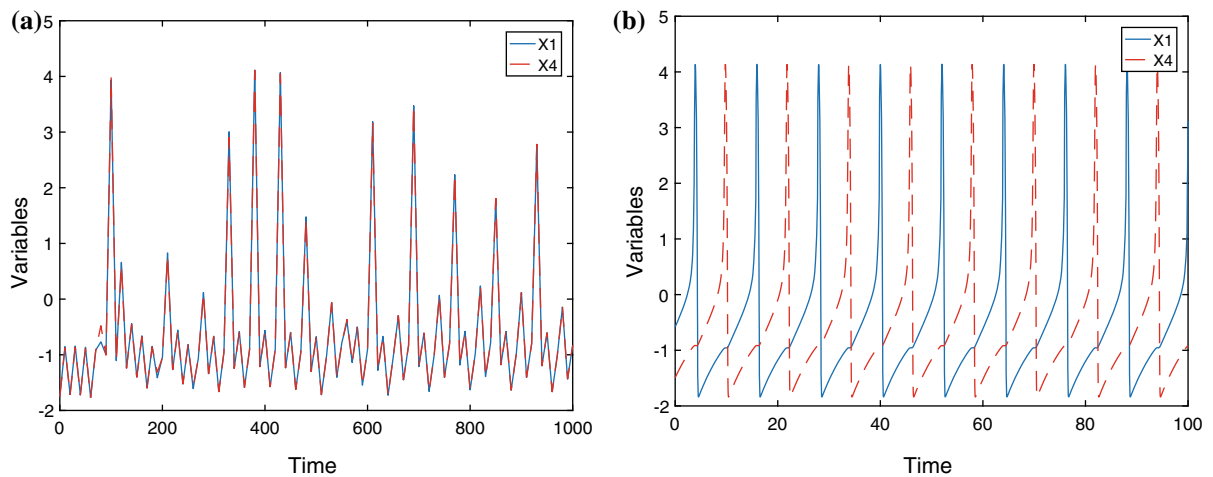


Fig. 1 Time series of the first variables (x_1 and x_4) of indirect and synaptic coupled neurons. **a** At $\varepsilon = 1$, $\omega_2 = 0$, the synchronization behaviour of two neurons is established. **b** Time

series of indirect and synaptic coupled neurons exhibits anti-phase synchronization for the values of coupling strengths $\varepsilon = 0$ and $\omega_2 = 1$

There is excitatory or inhibitory synaptic coupling depending upon whether the synapse is fast or slow [36]. Direct synapses are activated as soon as a membrane potential crosses the threshold value, while the effect of indirect synapse is to introduce a delay from the time one oscillator jumps up until the time the other feels the synaptic input.

2.2 Time series plots for linear indirect synaptic coupling

The effects of synaptic coupling on the time series behaviour of neurons are examined. The chaotic behaviour of indirect synaptic coupled neurons depends on the specific values of parameters in the H–R neuron equation.

2.2.1 Synchronization

Synchronization behaviour of two linear indirect synaptic coupled H–R neurons is shown through time series analysis. Here for sufficiently large value of one coupling parameter (ω_2), bursts of both neurons become synchronized as shown in Fig. 1a.

2.2.2 Anti-phase synchronization

Anti-phase synchronization property of linear indirect synaptic coupled neurons (Fig. 1b) is shown through

time series analysis. Here one of the parameters is of low value and other is of high value.

2.2.3 Amplitude death

For higher values of coupling parameters, amplitude death of indirect synaptic coupled neurons is established through time series analysis of first variables x_1 and x_4 (Fig. 2). Here oscillation of two neurons comes to a common steady-state condition.

We have also identified the regions of amplitude death, synchronization and anti-phase synchronization in the two neuron system for linear, indirect synaptic coupling with various values of coupling parameters (Fig. 3). The regions are identified by correlation analysis [9] where synchronization, anti-phase synchronization and amplitude death are found to emerge in. When one of the control or coupling parameters is set as high, synchronization or anti-phase synchronization regions are observed.

Due to rigorous mathematical calculations, stability analysis of synaptic coupled H–R neuron is not done.

2.3 Lyapunov exponent plot for synaptic coupled H–R neurons

The Lyapunov exponent (LE) plot for synaptic coupled system is shown in Fig. 4. The increased LE value reflects greater sensitivity to initial conditions

Fig. 2 Time series plots of indirect and synaptic coupled H–R neurons evolves into amplitude death condition for higher values of both of the coupling/control parameters ε and ω_2

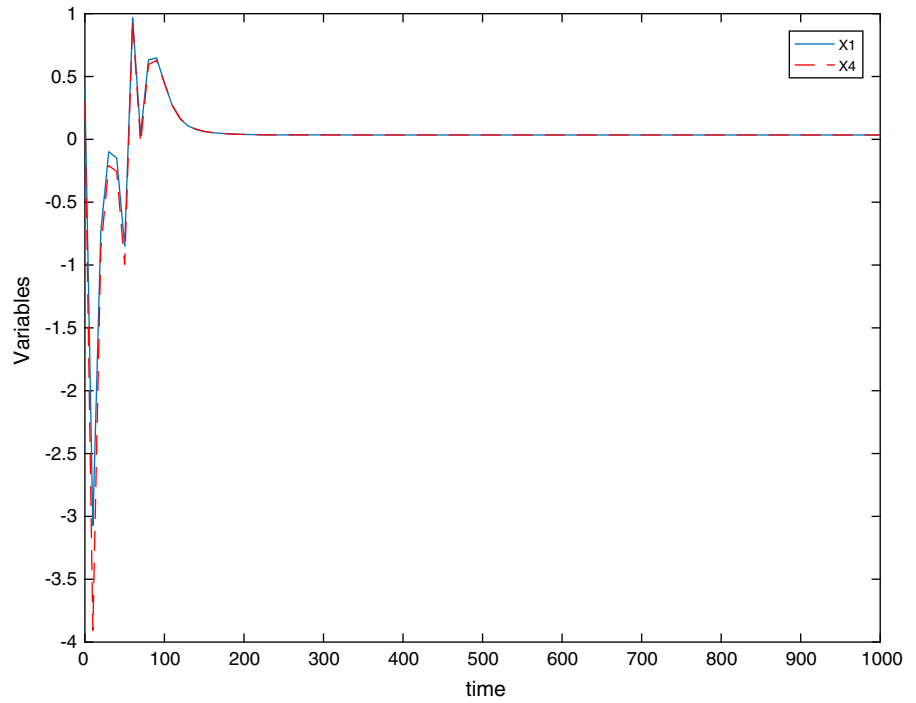


Fig. 3 Amplitude death, synchronization and anti-phase synchronization regions are shown through $\varepsilon - \omega_2$ plot. Regions are found by varying coupling strengths. Parameter range is selected as $\varepsilon = [0:0.5:5]$ and $\omega_2 = [0:0.2:1.2]$. Synchronization and anti-phase synchronization regions obtained are depicted through *yellow* and *dark blue* colour in the above plot. For higher values of control parameters amplitude death behaviour is set in, which is shown by *light green* region in the figure. (Color figure online)

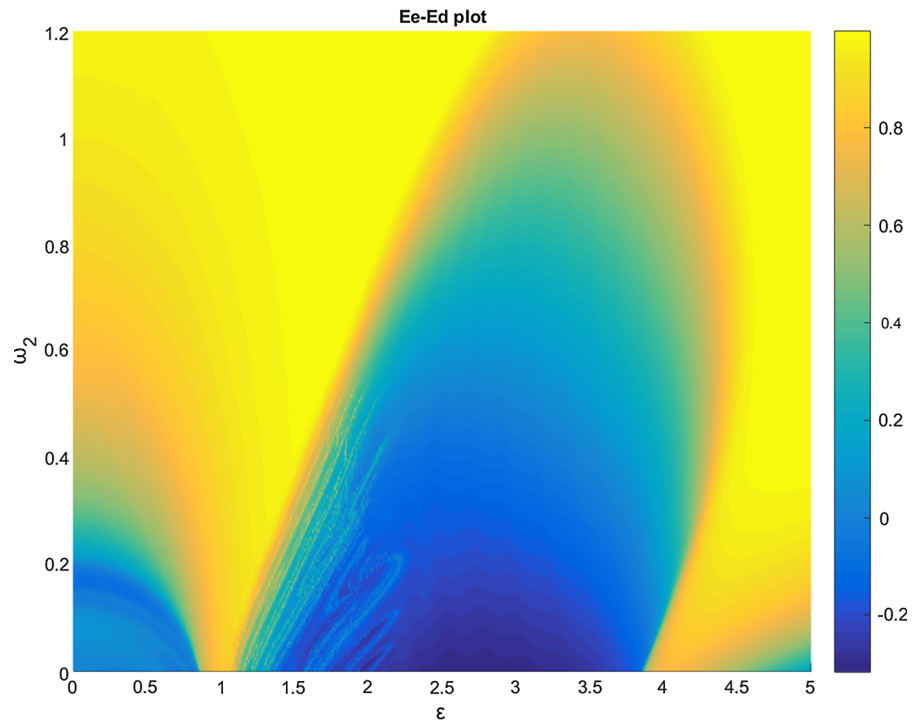
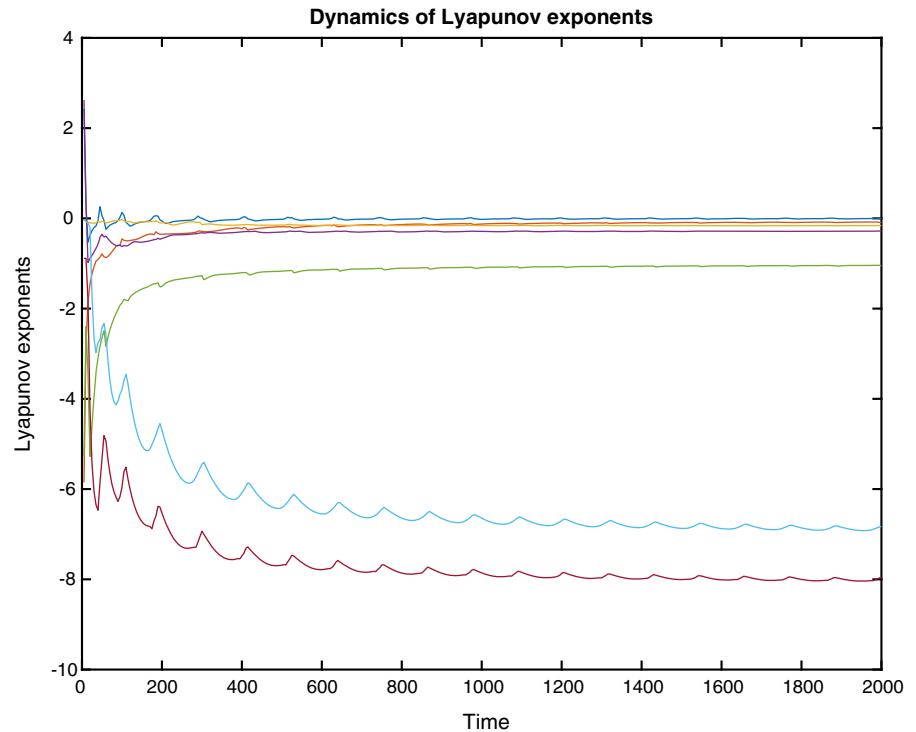


Fig. 4 Lyapunov exponent plot for linear synaptic coupled H–R neurons



and characterizes unpredictable variations, while low value indicates the regularity of the system.

3 Nonlinear feedback coupling in H–R neurons

In this section the dynamical behaviour of two H–R neurons is examined where cubic nonlinear coupling is adopted. The excitability in neuron-based excitable cells is most often associated with the presence of a cubic nonlinearity in the relevant system of differential equations. When the nonlinear coupling feedback term of cubic order is added to the differential equation representing dynamical evolution of first variable of H–R model, the two neurons do not achieve full synchronization. But when a quadratic form of membrane potential is added to the differential equation of fast current variable x_2 or x_5 [37], the behaviour of dynamics is interesting. It is found that the coupling strengths decide the evolution of the system.

In H–R neuron, the recovery variable which is the current variable x_2 is influenced by the outward flow of potassium ions immediately after the discharge of action potential. The potassium ion current slows down the returning of membrane potential to the thresh-

old value, and it also reduces frequency of repeating discharge. It also allows a delay between excitable simulate and action discharge. So introduction of the quadratic form of membrane voltage between two neurons results in a coupling feedback into the flow of potassium ions. This means a change of potassium ion concentration affects modulation with respect to the burst interval of H–R neurons which in turn may affect chaotic synchronization of two neurons [37].

Consider the nonlinear feedback coupled H–R neurons

$$\begin{aligned}
 \dot{x}_1 &= x_2 - ax_1^3 + bx_1^2 + I_{\text{ext}} - x_3 - \varepsilon (x_1^3 - x_4^3) \\
 \dot{x}_2 &= c - dx_1^2 - x_2 + \omega_2 (x_1^2 - x_4^2) \\
 \dot{x}_3 &= r (s (x_1 - x_0) - x_3) \\
 \dot{x}_4 &= x_5 - ax_4^3 + bx_4^2 + I_{\text{ext}} - x_6 - \varepsilon (x_1^3 - x_4^3) \\
 \dot{x}_5 &= c - dx_4^2 - x_5 + \omega_2 (x_4^2 - x_1^2) \\
 \dot{x}_6 &= r (s (x_4 - x_0) - x_6)
 \end{aligned} \tag{2}$$

Here the membrane potential of a neuron and the related ion currents across the membrane are represented by the variables x_1, x_2 and x_3 . Parameters a, b, c, d, r, s and I_{ext} are chosen as $a = 1, b =$

3, $d = 5$, $c = 1$, $r = 0.006$, $s = 4$ and $I_{ext} = 3.05$, and initial condition of the system is chosen such that $[x_1, x_2, x_3, x_4, x_5, x_6]$ are assigned the values $[0.3, 0.3, 3.0, 0.2, 0.35, 3.2]$ where ε and ω_2 are the coupling parameters. Here $\varepsilon(x_1^3 - x_4^3)$ represents nonlinear feedback of cubic order. By varying the value of coupling strength, various dynamics of chaotic neurons are analysed.

3.1 Linear stability analysis

We present an analysis of stability of the steady state of two H–R neurons coupled by nonlinear cubic feedback coupling.

$$\begin{aligned} \dot{x}_1 &= f(x_1) + \varepsilon(x_1^3 - x_4^3) \\ \dot{x}_2 &= f(x_2) + \omega_2(x_1^2 - x_4^2) \end{aligned} \tag{3}$$

$$\begin{aligned} \dot{x}_4 &= f(x_4) + \varepsilon(x_1^3 - x_4^3) \\ \dot{x}_5 &= f(x_5) + \omega_2(x_4^2 - x_1^2) \end{aligned} \tag{4}$$

Here ε and ω_2 are coupling parameters. Let $\bar{x}_1, \bar{x}_2, \bar{x}_4, \bar{x}_5$ be the steady state of the system, then $f(x_1, \bar{x}_1) = 0$, $f(x_2, \bar{x}_2) = 0$, $f(x_4, \bar{x}_4) = 0$, and $f(x_5, \bar{x}_5) = 0$.

Let $\eta_1, \eta_2, \eta_4, \eta_5$ be the infinitesimal perturbations of the system. As $\eta_1, \eta_2, \eta_4, \eta_5$ grows x_1, x_2, x_4 and x_5 move away from steady state and if these perturbation values of η decay to zero, the variable values of x_1, x_2, x_4 and x_5 move towards steady state.

To obtain stability of the steady state of systems, we write variational equations by linearizing above equations.

$$\dot{\eta}_1 = \dot{x}_1 = f(\bar{x}_1 + \eta_1)$$

Using Taylor expansion and neglecting higher-order terms,

$$\dot{\eta}_1 = \eta_1 f'(x_1, \bar{x}_1)$$

From Eqs. (3) and (4) we get

$$\begin{aligned} \dot{\eta}_1 &= f'(x_1) \eta_1 + \varepsilon(\eta_1^3 - \eta_4^3) \\ \dot{\eta}_4 &= f'(x_4) \eta_4 + \varepsilon(\eta_1^3 - \eta_4^3) \end{aligned} \tag{5}$$

Let the synchronization and anti-synchronization tendencies are expressed through the variables η_{syn} and η_{anti} , respectively. Then $\eta_{syn} = \eta_1 - \eta_4$ and $\eta_{anti} = \eta_1 + \eta_4$,

$$\begin{aligned} \dot{\eta}_{syn} &= \dot{\eta}_1 - \dot{\eta}_4 \\ \dot{\eta}_{anti} &= \dot{\eta}_1 + \dot{\eta}_4 \end{aligned} \tag{6}$$

So condition for synchronization is obtained as

$$\begin{aligned} \dot{\eta}_{syn} &= \left[\frac{f'(x_1) + f'(x_4)}{2} \right] \eta_{syn} \\ &+ \left[\frac{f'(x_1) - f'(x_4)}{2} \right] \eta_{anti} \\ &+ \varepsilon(\eta_1^3 - \eta_4^3 - \eta_1^3 + \eta_4^3) \end{aligned}$$

Considering the time average value of $f'(x_1)$ and $f'(x_4)$ is approximately the same and is replaced by effective constant value τ , the equation changes as

$$\dot{\eta}_{syn} = \tau \eta_{syn} \tag{7}$$

From Eq. (7), it is clear that cubic order feedback alone doesn't give a complete synchronization.

Similarly for the other set of variables x_2 and x_5 the condition becomes

$$\begin{aligned} \dot{\eta}_{syn} &= \dot{\eta}_2 - \dot{\eta}_5 \\ &= \tau \eta_{syn} + 2\omega_2(\eta_1^2 - \eta_4^2) \end{aligned} \tag{8}$$

From Eq. (8), it is clear that synchronization is achieved through the term $2\omega_2(\eta_1^2 - \eta_4^2)$. This is in agreement with numerical analysis of the coupling scheme.

Anti-synchronization properties are obtained for the system through the same analysis described above.

$$\begin{aligned} \dot{\eta}_{anti} &= \dot{\eta}_1 + \dot{\eta}_4 \\ &= \tau \eta_{anti} + 2\varepsilon(\eta_1^3 - \eta_4^3) \\ &= \tau \eta_{anti} + 2\varepsilon \cdot \eta_{syn}(\eta_1^2 + \eta_1 \eta_4 + \eta_4^2) \end{aligned} \tag{9}$$

Second term in the above equation leads to anti-synchronization.

Similarly, the corresponding equations for variables x_2 and x_5 lead to

$$\begin{aligned} \dot{\eta}_{anti} &= \dot{\eta}_2 + \dot{\eta}_5 \\ &= \tau \eta_{anti} \end{aligned} \tag{10}$$

From Eqs. (9) and (10) Jacobian matrix is written as

$$J = \begin{pmatrix} \tau & 0 \\ 2\varepsilon(\eta_1^2 + \eta_1 \eta_4 + \eta_4^2) & \tau \end{pmatrix}$$

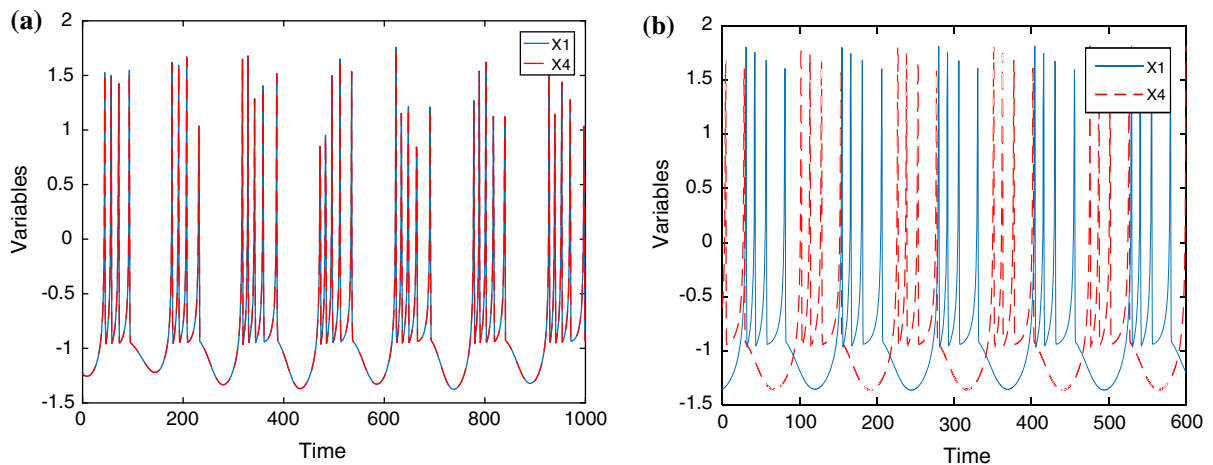


Fig. 5 **a** Time series plots of first variables show synchronization of coupled neurons. Bursting synchronization of neurons with nonlinear feedback in cubic order is obtained for $\varepsilon = 1$, $\omega_2 = 1$, and $I_{\text{ext}} = 3.05$. **b** Time series plots of first variables shows

anti-phase synchronization of coupled neurons with cubic nonlinear feedback with parameter values $\varepsilon = 0$, $\omega_2 = 0.001$, and $I_{\text{ext}} = 3.00$

Jacobian value for Eqs. (5) and (7) is also calculated, eigenvalues obtained may be real which is positive or negative, and the corresponding fixed point is of stable node or unstable node.

Eigen values of the above are

$$\lambda = \tau \mp \sqrt{\tau^2 + 8\varepsilon\tau(\eta_1^3 - \eta_4^3)} \quad (11)$$

Anti-synchronization and synchronization tendencies are effective when corresponding the Lyapunov exponents, i.e. if the real parts of the eigenvalues are negative. So condition for stability is obtained as $\eta_1^3 > \eta_4^3$.

3.2 Time series plot of coupled neurons with cubic order feedback

3.2.1 Synchronization

Synchronization of two nonlinear cubic feedback coupled H–R neurons is shown through time series analysis. As nonlinear coupling replaces linear coupling, the synchronization pattern given in Fig. 1a changes to behaviour shown in Fig. 5a which shows synchronization of first variables for $I_{\text{ext}} = 3.05$. The bursting behaviour for synchronization exhibited by the H–R system is an additional feature shown by the presence of nonlinear coupling.

3.2.2 Anti-phase synchronization

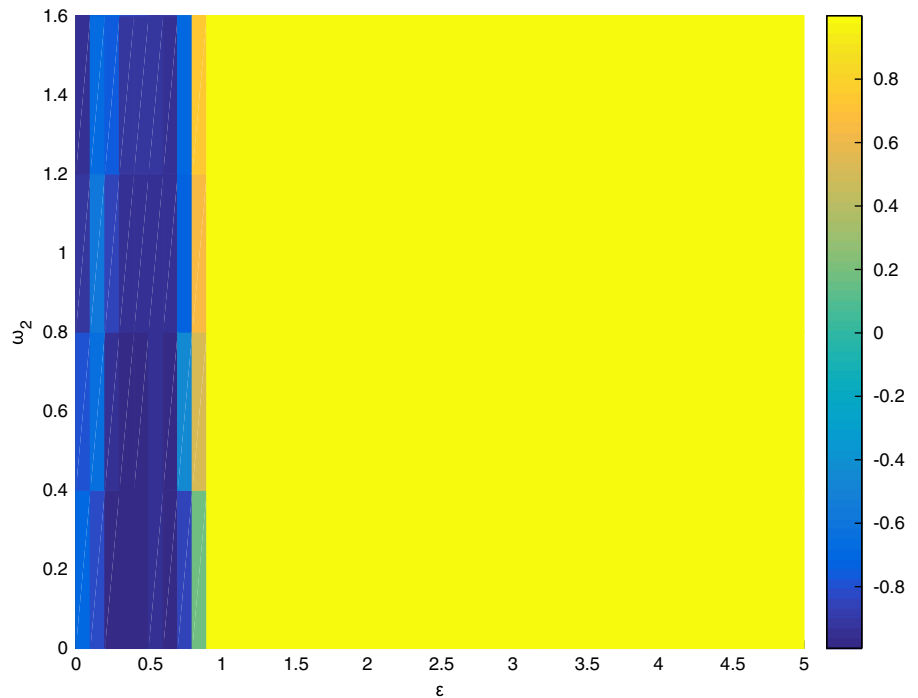
The anti-phase synchronization of nonlinear cubic feedback coupled neurons is established through time series analysis for certain values of coupling parameters and current. Here first variables of two coupled H–R neurons are showing anti-phase properties, which are depicted through blue and red colour as shown in Fig. 5b. The plot is obtained for the parameter values $\varepsilon = 0$, $\omega_2 = 0.001$, and $I_{\text{ext}} = 3.00$.

The regions of synchronization, anti-phase synchronization and amplitude death for different ranges of control parameters are depicted in Fig. 6. Here control or coupling parameters are selected in the range $\varepsilon = [0:0.5:5]$ and $\omega_2 = [0:0.2:1.6]$.

3.3 Lyapunov exponent plot for nonlinear cubic feedback coupling in H–R neurons

The behaviour of nonlinear cubic feedback coupled H–R neuron is analysed through Lyapunov exponent (LE) plot which is found to exhibit similar behaviour as in Fig. 4. Here the low LE values indicate regularity of the coupling method. Largest LE is obtained in the range -1.1834 to -1.1832 . It is in agreement with synchronization stability of this system observed by Fang [37].

Fig. 6 Anti-phase synchronization, synchronization and amplitude death of cubic feedback coupled neurons are examined through $\varepsilon - \omega_2$ plot. When the value of $\varepsilon = [.9:0.5:5]$ and $\omega_2 = [0 : 0.5 : 1.6]$, synchronization regions are observed and is shown by yellow colour in the figure. For the range $\varepsilon = [0:0.5:0.7]$ and $\omega_2 = [0 : 0.5 : 1.6]$, dark blue region shows anti-synchronization. Also for the values of $\varepsilon = [0.75:0.5:0.89]$ and $\omega_2 = [0:0.5:0.4]$, amplitude death is observed, depicted by light green. (Color figure online)



4 Memristor-based coupling in neurons

In 1971, Chua postulated the fourth basic circuit element memristor [38, 39] and established a missing constitutive relationship between the electrical charge and the magnetic flux. Using Lewis Carroll’s portmanteau naming technique [40], Chua named this hypothetical nonlinear device as memristor (memory + resistor). It demonstrated the hysteresis property of the ferromagnetic core memory and also the dissipative characteristics of a resistor. Clearly, in such devices, the nonlinear resistance can be memorized indefinitely by controlling the flow of the electrical charge or the magnetic flux [41].

Memristor are nanoscale devices. Although memristor and memristive systems have been introduced a long time ago by Chua, applications of them have developed recently after the invention of the nanoscale HP memristor [42].

A memristor consists of a variable resistance and has two terminals. In DRAM a memristor can replace the capacitor which can store one bit of data. Then this memory is not volatile, has no leakage power and at the same time is more stable. Also in comparison with flash memory, this memory has improved speed and scalability. A memristor can also connect electric charge

to magnetic flux. As its resistive value is retained, it can increase flow of current in one direction and can decrease flow of current in the opposite direction.

Memristor finds improved applications [43] in logic circuits and in digital memory. In neuromorphic systems they can act as basic building blocks where they behave like biological synapses. Neurons and synapses act as electronic systems. Besides being the basis of next-generation ultra dense non-volatile memories, a nanoscale memristor also has the potential to reproduce the behaviour of a biological synapse. As in a living creature the weight of a synapse is adapted by the ionic flow through it, so the conductance of a memristor is adjusted by the flux across or the charge through it depending on its controlling source [16].

In the following sections we consider two Hindmarsh–Rose neurons, coupled via a memristive device mimicking a biological synapse. We investigate how the dynamics of the memristive element may influence the synchronization and other interesting properties.

4.1 Memristor controlled by cubic order flux

The proposed memristor is having cubic nonlinearity which is represented by $q(\varphi) = \alpha\varphi + \beta\varphi^3$. It is a

smooth continuous cubic function, and the corresponding memductance is $W(\varphi) = \alpha + 3\beta\varphi^2$. It is used as a memristive coupling term and will act as an artificial synapse between coupled neuron cells. Hence, they are responsible for chaotic dynamics of the system. Flux-controlled memristor is used to emulate the excitatory and inhibitory synaptic connection between the neurons [16]. It is used as a memristive coupling term and will act as artificial synapse between coupled neuron cells.

Consider the memristive mutual coupled H–R equations as given below

$$\begin{aligned}\dot{x}_1 &= x_2 - ax_1^3 + bx_1^2 + I_{\text{ext}} - x_3 \\ &\quad - (\alpha + \beta u^2)(x_1 - x_4) \\ \dot{x}_2 &= c - dx_1^2 - x_2 \\ \dot{x}_3 &= r(s(x_1 - x_0) - x_3) \\ \dot{x}_4 &= x_5 - ax_4^3 + bx_4^2 + I_{\text{ext}} - x_6 \\ &\quad - (\alpha + \beta u^2)(x_4 - x_1) \\ \dot{x}_5 &= c - dx_4^2 - x_5 \\ \dot{x}_6 &= r(s(x_4 - x_0) - x_6) \\ \dot{u} &= x_1 - x_4\end{aligned}\quad (12)$$

The variable x_1 represents the membrane potential of a neuron, and the variables x_2 and x_3 are related ion currents across the membrane. Here parameters are taken as $a = 1$, $b = 3$, $d = 5$, $c = 1$, $r = 0.005$, $s = 4$ and $k = 1$. x_1 and x_4 gives the coupling between the neurons achieved through memristor. u is flux variable due to memristor. Here the memductance term $(\alpha + \beta u^2)$ functions as cubic flux-controlled memristive term and acts as coupling synapse between two neurons.

4.1.1 Linear stability analysis

We present the analysis of stability of the steady state of two H–R neurons coupled by cubic flux-controlled memristor.

$$\begin{aligned}\dot{x}_1 &= f(x_1) - c(\alpha + \beta u^2)(x_1 - x_4) \\ \dot{x}_4 &= f(x_4) + c(\alpha + \beta u^2)(x_1 - x_4) \\ \dot{u} &= (x_1 - x_4)\end{aligned}\quad (13)$$

Here α and β are coupling parameters and c is a constant. Let \bar{x}_1 , \bar{x}_4 and \bar{u} represent the steady state of the system, then $f(x_1, \bar{x}_1) = 0$, $f(x_4, \bar{x}_4) = 0$ and $f(u, \bar{u}) = 0$.

Let η_1 , η_4 and u be the infinitesimal perturbations of the system. As η_1 , η_4 and z grow, x_1 , x_4 and u move away from steady state and if the values of η_1 , η_4 and z decay to zero, x_1 , x_4 and u move towards steady state.

To obtain stability of the steady state of two systems, we write variational equations formed by linearizing equation for x_1 as

$$\dot{\eta}_1 = \dot{x}_1 = f(\bar{x}_1 + \eta_1)$$

Using Taylor expansion and neglecting higher-order terms,

$$\begin{aligned}\dot{\eta}_1 &= \eta_1 f'(x_1, \bar{x}_1) \\ \dot{\eta}_1 &= f'(x_1) \eta_1 - c(\alpha + \beta u^2)(x_1 - x_4) \\ \dot{\eta}_4 &= f'(x_4) \eta_4 + c(\alpha + \beta u^2)(x_1 - x_4)\end{aligned}\quad (14)$$

Let the synchronization and anti-synchronization tendencies are expressed through the variables η_{syn} and η_{anti} , respectively. Then $\eta_{\text{syn}} = \eta_1 - \eta_4$ and $\eta_{\text{anti}} = \eta_1 + \eta_4$

$$\dot{\eta}_{\text{syn}} = \dot{\eta}_1 - \dot{\eta}_4 \quad (15a)$$

$$\dot{\eta}_{\text{anti}} = \dot{\eta}_1 + \dot{\eta}_4 \quad (15b)$$

From Eqs. (13) and (15a),

$$\begin{aligned}\dot{\eta}_{\text{syn}} &= \left[\frac{f'(x_1) + f'(x_4)}{2} \right] \eta_{\text{syn}} \\ &\quad + \left[\frac{f'(x_1) - f'(x_4)}{2} \right] \eta_{\text{anti}} \\ &\quad - 2c(\alpha + \beta u^2) \eta_{\text{syn}}\end{aligned}\quad (16)$$

Considering that the time average value of $f'(x_1)$ and $f'(x_4)$ are approximately the same and replaced by effective constant value τ , equation changes as

$$\dot{\eta}_{\text{syn}} = \tau \eta_{\text{syn}} - 2c(\alpha + \beta u^2) \eta_{\text{syn}} \quad (17a)$$

Similarly, we get

$$\dot{\eta}_{\text{anti}} = \tau \eta_{\text{anti}} \quad (17b)$$

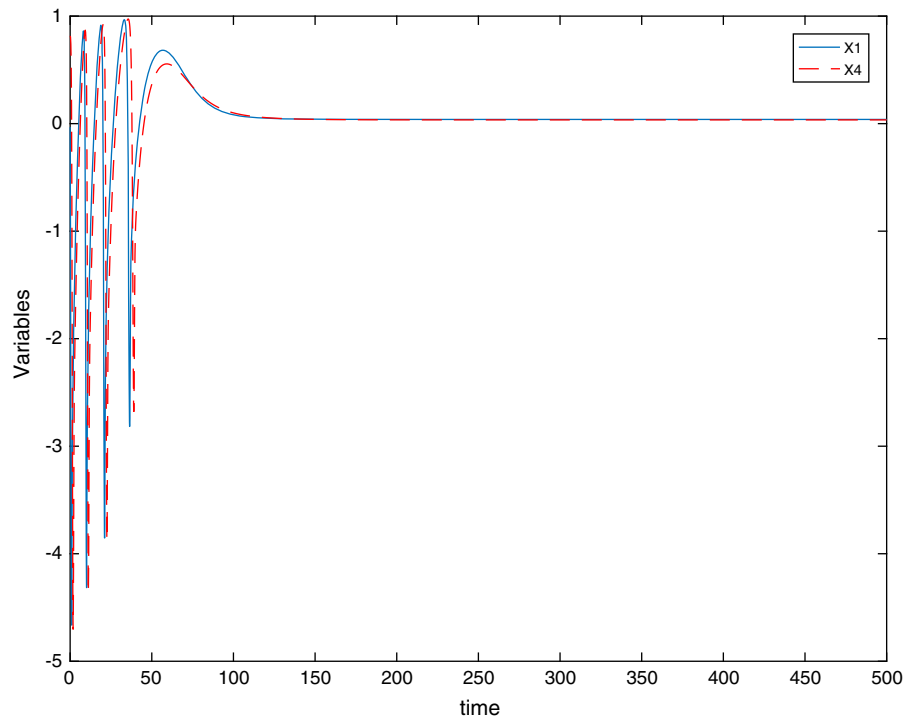
$$\dot{u} = c \eta_{\text{syn}} \quad (17c)$$

From Eq. (17a) Lyapunov exponent is obtained as

$$\lambda = \tau - 2c(\alpha + \beta u^2) \quad (18)$$

The synchronization and anti-synchronization tendencies are effective when corresponding the Lyapunov

Fig. 7 Time series plots of first variables x_1 and x_4 of cubic flux-controlled memristor shows amplitude death state. When the parameter values are set as $\alpha = 0.005$, $\beta = 0$ and $I_{\text{ext}} = 3$ amplitude death states of neurons are emerging out



exponents, i.e. real part of eigenvalues are negative. So condition for stability is given as below.

$$\beta > \frac{\tau}{2cu^2} - \alpha \tag{19}$$

These synchronization conditions are compatible with the numerical computations. Also the anti-synchronization properties are not exactly observed for memristor coupled systems. It is also evident from Eq. (17b).

4.1.2 Time series plots with cubic flux-controlled memristor

Bidirectional coupling In bidirectional coupling both the neurons are influenced by a memristor of cubic order flux. Synchronization and amplitude death behaviour are exhibited by the system as described below.

Synchronization behaviour in bidirectional coupling

Synchronization of H–R neurons coupled by cubic flux-controlled memristor shows chaotic bursting synchronization for the parameters $a = 1$, $b = 3$, $d = 5$, $c = 1$, $\alpha = 0.05$, $\beta = 0.5$ and $I_{\text{ext}} = 3$. Time series plots of first variables x_1 and x_4 shows synchronization

pattern where the number of spikes per burst is irregular. The dynamics exhibited are very similar to that of coupled neurons with cubic order feedback, and it is as shown in Fig. 5a.

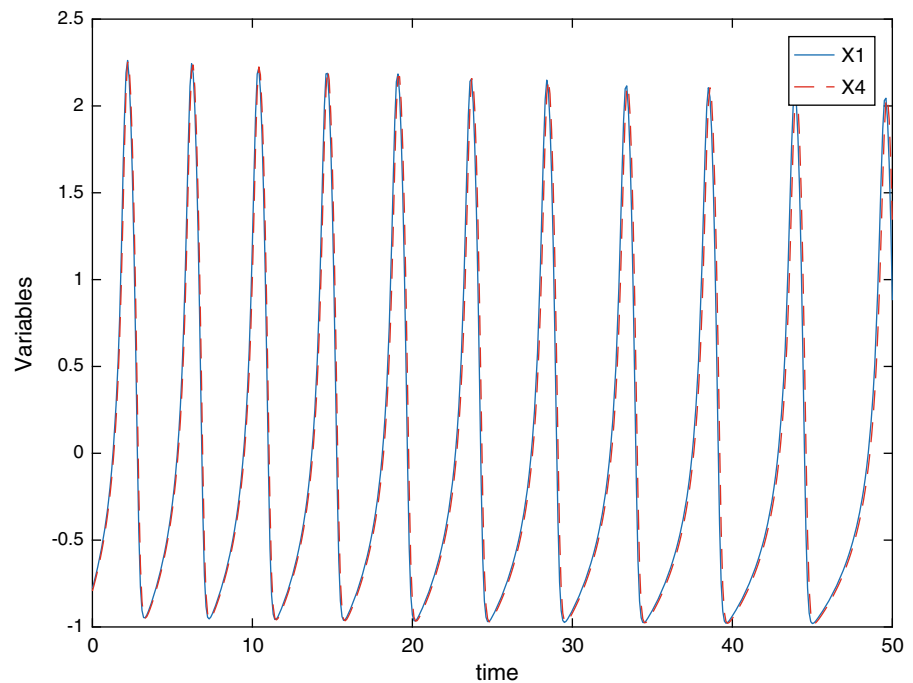
Amplitude death

As the values of α , β and current are changed, time series plots of cubic flux-controlled memristor coupled H–R neurons shows the amplitude death state as shown in Fig. 7. Here first variables of coupled H–R neurons come to a common steady state which was unstable otherwise. The parameter values are set as $\alpha = 0.005$, $\beta = 0$ and $I_{\text{ext}} = 3$.

Unidirectional coupling

In unidirectional coupling only one neuron is triggered by a memristor of cubic order flux while the other neuron is not influenced by coupling. In the scenario represented by Eq. (12), as the bidirectional coupling is replaced with unidirectional coupling of cubic flux-controlled memristor, the x_1 variable (the membrane potential of first neuron) is not influenced by the term $(\alpha + \beta u^2)(x_1 - x_4)$. The dynamics observed are shown in Figs. 8–11.

Fig. 8 Time series plots of first variables x_1 and x_4 shows synchronization pattern in unidirectional coupled cubic flux-controlled memristor. The parameters are chosen as $\alpha = 0.001$, $\beta = 0.02$, and $I_{\text{ext}} = 2.8$ where tonic synchronization pattern of neurons is exhibited



Synchronization behaviour in unidirectional coupling

Synchronization pattern of two H–R neurons coupled with unidirectional cubic flux-controlled memristor is shown (Fig. 8) through time series analysis. Here bursting synchronization of bidirectional coupling is replaced by the tonic spiking in unidirectional coupling. As the neuron is stimulated, the inhibitory ion currents will dominate the stimulating current and corresponding membrane potential will decrease. Persistence of this activity leads to tonic spiking. The plot is obtained for the parameter values $\alpha = 0.001$, $\beta = 0.02$ and $I_{\text{ext}} = 2.8$.

Tonic spiking of one neuron and the inactive state of the other neuron in unidirectional coupling

Time series analysis of two H–R neurons coupled with unidirectional cubic flux-controlled memristor leads to tonic spiking for one of the neurons and inactive or death states for the uncoupled neuron as shown in Fig. 9.

Bursting and death of neuron

As the parameters are changed, the tonic spiking gives way to bursting for the coupled neuron while the uncoupled neuron remains in the resting state for H–R neu-

rons coupled with unidirectional cubic flux-controlled memristor. The dynamics are established through time series plots (Fig. 10) for the parameter values $\alpha = 0.02$, $\beta = 0$ and $I_{\text{ext}} = 5$.

Anti-phase dynamics

For still other parameter values it is interesting to report anti-phase synchronization of two H–R neurons with unidirectional coupled cubic flux-controlled memristor as shown in Fig. 11. Here bursting behaviour of two neurons shows anti-phase dynamics. To obtain the desired plot, parameter values are set as $\alpha = 0.02$, $\beta = 0.3$ and $I_{\text{ext}} = 2.8$.

4.1.3 Lyapunov exponent plot

The dynamics of Lyapunov exponents for H–R neurons coupled with cubic flux-controlled memristor are shown in Fig. 12. It is observed that largest LE value is close to 1 (0.9727). Positive value of LE's obtained due to coupling has much importance. The arterial blood pressure time series and ocular aberration dynamics of human eye exhibit positive Lyapunov exponents. So our coupling scheme can be referred to some neural base system analysis.

Fig. 9 Time series plots of the first variables x_1 and x_4 of the two coupled neurons. Here the coupling is unidirectional through flux-controlled memristor. With parameter values $d = 2.82$, $\alpha = 1$, $\beta = 0.01$ and $I_{ext} = 4$ tonic spiking is shown up for one neuron and inactive or death state is exhibited by the uncoupled neuron

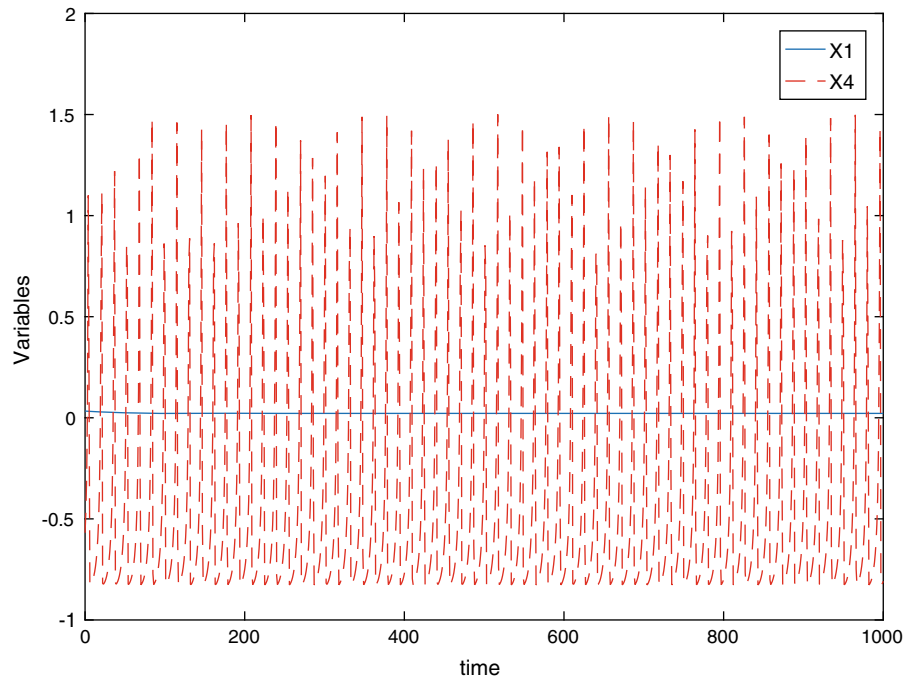
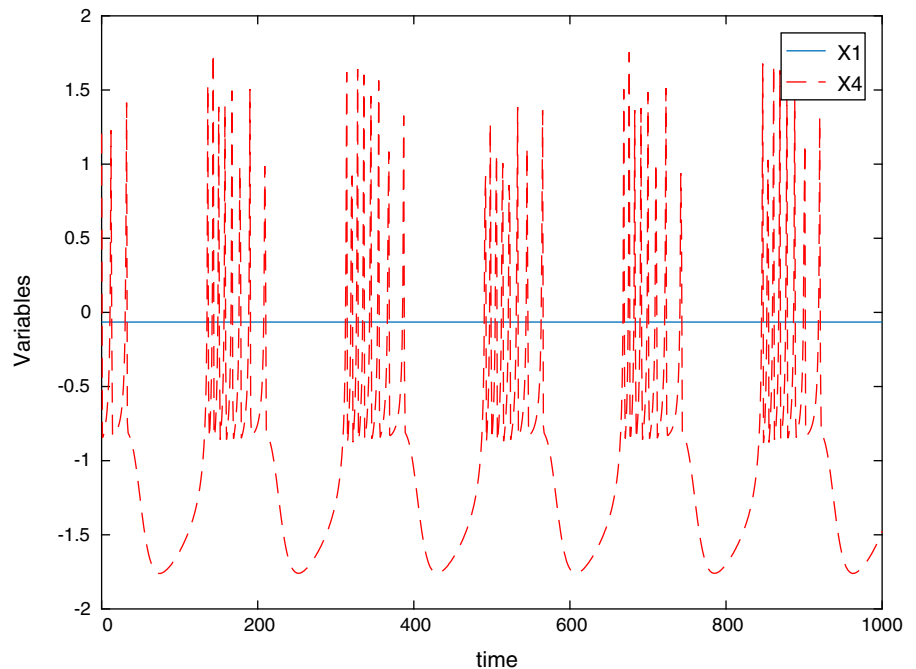


Fig. 10 Time evolution of first variables x_1 and x_4 for unidirectional coupled cubic flux-controlled memristor. As the parameter is changed to $\alpha = 0.02$, $\beta = 0$ and $I_{ext} = 5$, coupled neuron exhibits the bursting but the other neuron seems to be inactive



4.2 Memristor controlled by quadratic flux

In this section, the properties of memristor controlled by quadratic flux with varying coupling strengths and external currents are studied. For the quadratic flux-

controlled memristor [45] studied in this section, the memristance can be expressed as:

$$M(\phi) = \alpha\phi^2 + \beta\phi + \gamma \tag{20}$$

Fig. 11 Time series plots of first variables x_1 and x_4 shows anti-phase synchronization in unidirectional coupling by cubic flux-controlled memristor. Anti-phase dynamics obtained above have some similarity with that of time series plot of firing pattern of autaptic neuron [44]. Parameters are chosen as $\alpha = 0.02$, $\beta = 0.3$ and $I_{\text{ext}} = 2.8$

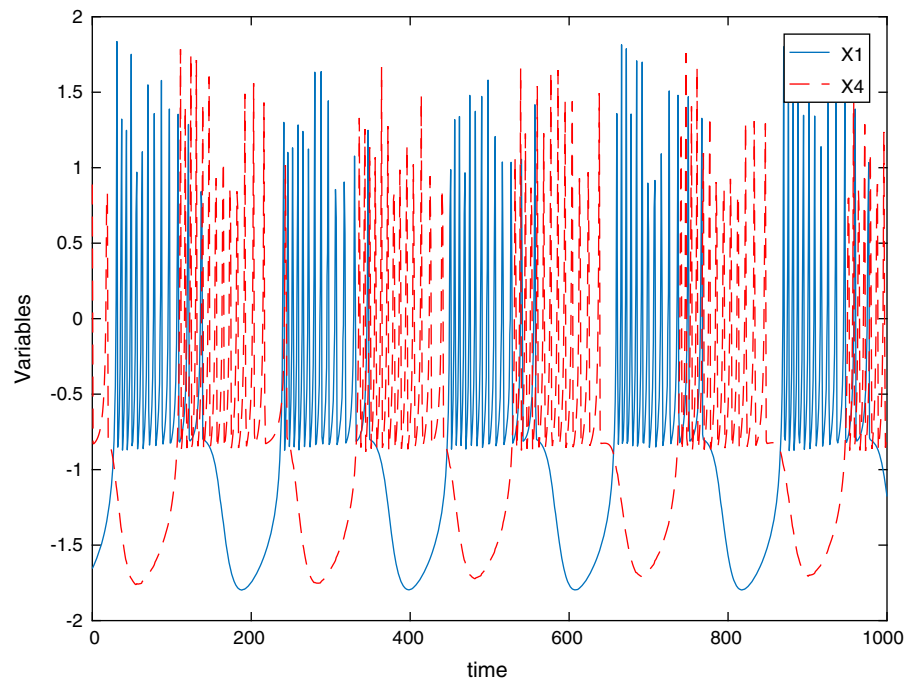
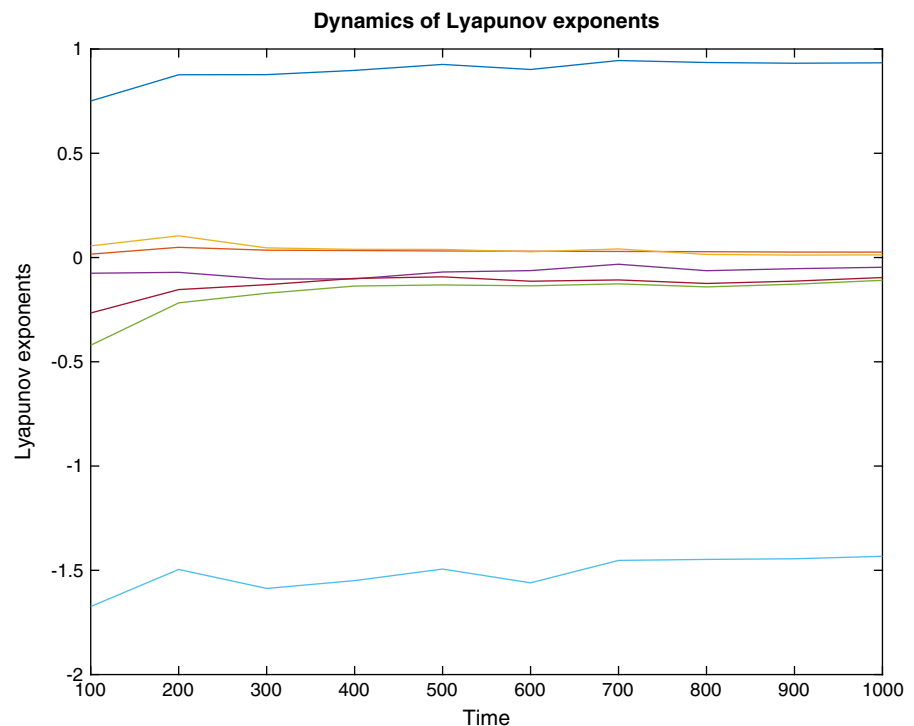


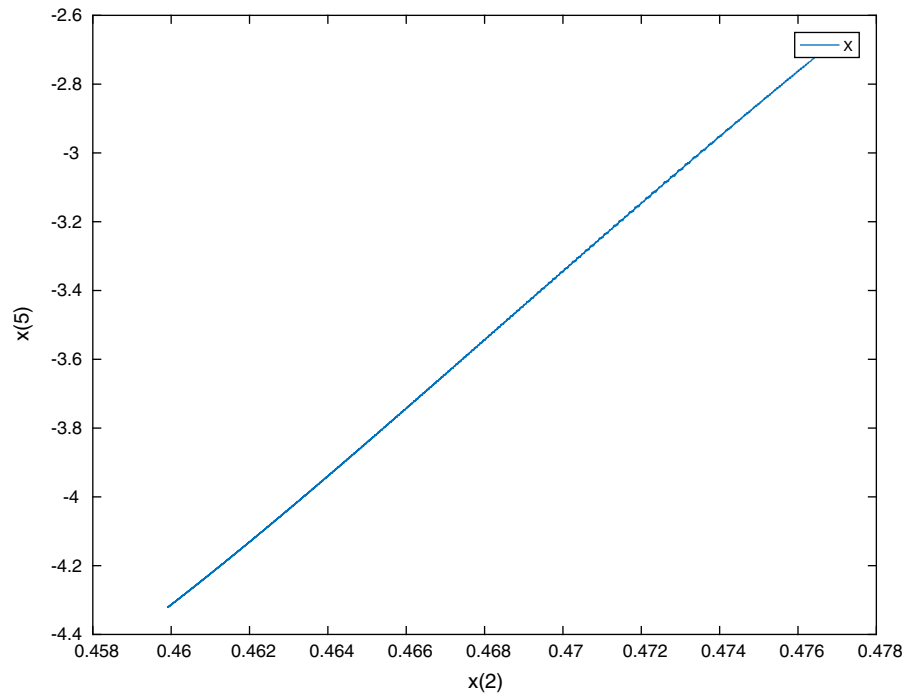
Fig. 12 Lyapunov exponent plot for H–R neurons coupled by cubic flux-controlled memristor



We can see that $M(\phi)$ is linear flux-controlled as $\alpha = 0$. Memristor of this type has been researched widely, so we focus on the influence of quadratic type coupling in H–R neuron.

$$\begin{aligned} \dot{x}_1 &= x_2 - ax_1^3 + bx_1^2 + I_{\text{ext}} - x_3 \\ &\quad - (\alpha\phi^2 + \beta\phi + \gamma)(x_1 - x_4) \\ \dot{x}_2 &= c - dx_1^2 - x_2 \end{aligned}$$

Fig. 13 Phase portrait of second variables x_2 and x_5 shows synchronization pattern for the system of neurons coupled by memristor controlled by quadratic flux. Synchronization is observed for the parameters $\alpha = 2, \beta = 1, \gamma = 1$ and $I_{\text{ext}} = 2$



$$\begin{aligned}
 \dot{x}_3 &= r (s (x_1 - x_0) - x_3) \\
 \dot{x}_4 &= x_5 - ax_4^3 + bx_4^2 + I_{\text{ext}} \\
 &\quad - x_6 - (\alpha\phi^2 + \beta\phi + \gamma) (x_4 - x_1) \\
 \dot{x}_5 &= c - dx_4^2 - x_5 \\
 \dot{x}_6 &= r (s (x_4 - x_0) - x_6) \\
 \dot{u} &= x_1 - x_4
 \end{aligned}
 \tag{21}$$

The variable x_1 represents the membrane potential of a neuron, and the variables x_2 and x_3 are related ion currents across the membrane. Here parameters are taken as $a = 1, b = 3, d = 5, c = 1, r = 0.005, s = 4$ and $k = 1$. The term $M(\phi) = \alpha\phi^2 + \beta\phi + \gamma$ acts as quadratic memristive function and is used as coupling term.

4.2.1 Linear stability analysis

As in Sect. 4.1.1, we can do linear stability analysis of quadratic flux-controlled memristor. Then the condition for stability in quadratic flux-controlled memristor is

$$\beta > \left(\frac{\tau - A}{2C\phi} - \alpha\phi \right)
 \tag{22}$$

4.2.2 Phase portraits and time series plots of memristor coupled neurons controlled by quadratic flux

Synchronization Synchronization of two H–R neurons coupled with quadratic flux-controlled memristor is shown through the $x_2 - x_5$ plot. Parameter values are selected as $\alpha = 2, \beta = 1, \gamma = 1$ and $I_{\text{ext}} = 2$. Here two neurons behave in the same way and full synchronization is achieved as shown in Fig. 13.

Oscillation death Time series of two variables x_1 and x_4 of H–R neurons coupled with quadratic flux-controlled memristor shows oscillation death for the parameter values $\alpha = 1, \beta = 0, \gamma = 1$ and $I_{\text{ext}} = 1.4$. The coupled two neurons takes a stable rest state as depicted in Fig. 14.

Near-death spikes For some parameter values an interesting dynamic is exhibited by the H–R neurons which are coupled via quadratic flux-controlled memristor. Rare spikes are observed with time variation of variables of two neurons before death (near-death rare spikes [46–48]). Experimentally, it is observed that a few moments before death, the patients experience a burst in brain wave activity, with the spikes occur-

Fig. 14 Time series plots of first variables x_1 and x_4 of neurons with quadratic flux-controlled memristor. With parameter values $\alpha = 1, \beta = 0, \gamma = 1$ and $I_{\text{ext}} = 1.4$, oscillation deaths of neurons which are coupled by memristor governed by quadratic flux are shown

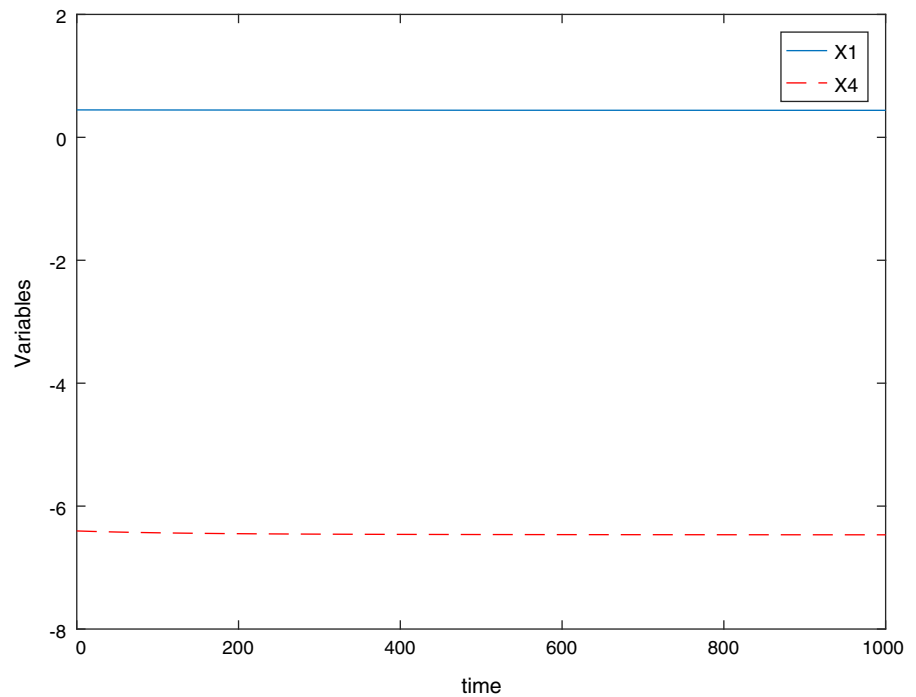
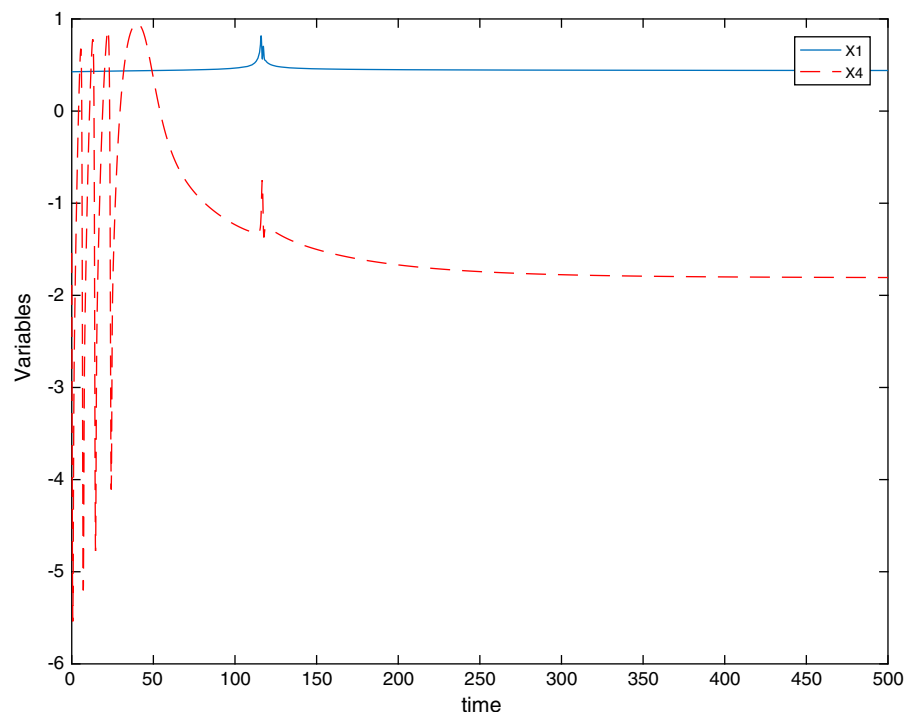


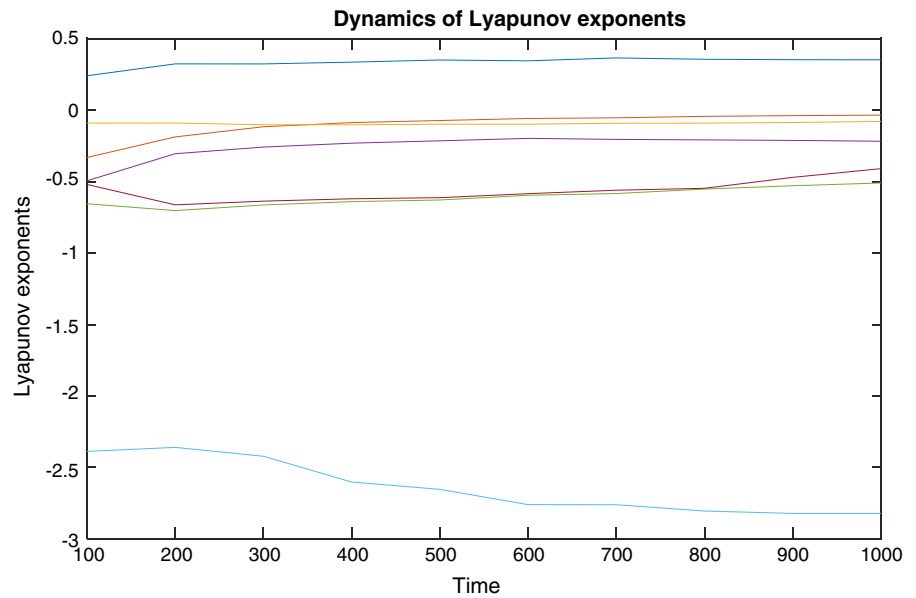
Fig. 15 Time series plots of first variables x_1 and x_4 of neurons with quadratic flux-controlled memristor. Dynamics obtained for parameter values $\alpha = 5, \beta = 1, \gamma = 0$ and $I_{\text{ext}} = 4$ and $\alpha = 2, \beta = 1, \gamma = 0$ and $I_{\text{ext}} = 3$ show phenomena like near-death rare spikes



ring simultaneously for two coupled neurons and with approximately of same intensity and of same duration. In Fig. 15 the behaviour is shown around the time slot 125.

The near-death spikes are supported by experimental observation [46–48]. Experimentalists implanted several electrodes across the brains of nine rats to measure their brain waves—rhythmic pulses of neural activity

Fig. 16 Lyapunov exponent plot for H–R neurons coupled with quadratic flux-controlled memristor



depending on their frequency. The rats were sedated with anaesthetic drugs, and then killed with either by a lethal injection that stopped their hearts, or by a fatal dose of carbon dioxide, after the hearts have stopped, most of these brainwaves weakened with time. But one set of waves, the *low-gamma* waves produced when neurons fire between 25 and 55 times per second, became *stronger* for a brief period. The activity in different parts of their brains also become more synchronized. Their low-gamma waves were synchronized when they were in their near-death state than when they were anaesthetized or awoken [46–48].

4.2.3 Lyapunov exponent plot

Lyapunov exponent plot for H–R neurons coupled with quadratic flux-controlled memristor dynamics is shown through Fig. 16. Sensitivity to initial condition of systems and its regularity are examined through plot.

4.3 Memristor controlled by exponential flux

The cubic flux-controlled memristor have limitations in situations which demand a larger current [49] and is not compatible with terminal voltage fluctuations. Here the memductance or memristance always keep increasing or decreasing until polarity of voltages or current reverses. The proposed exponential model obeys stable variation law of the memductance (memristance)

under various excitation voltages [49], and hence, this model meets large current situations. So the memristor controlled by exponential flux is chosen for coupling.

A novel model of the flux-controlled memristor is selected as below

$$q(\phi) = kb(a^{bq} - 1) \tag{23}$$

where $a > 0$ and $kba > 0$. Then, the memductance function of this memristor can be given by

$$W(\phi) = a^{bq} k \ln a \tag{24}$$

when $b < 0$, above equation model is a decremented flux-controlled memristor, that is, it’s memductance is monotonically decreasing (increasing) when the supply voltage is positive (negative). On the contrary, when $b > 0$, equation represents an incremental flux-controlled memristor.

Consider the exponential flux-controlled H–R model equations as

$$\begin{aligned} \dot{x}_1 &= x_2 - x_1^3 + b_1 x_1^2 + I_{\text{ext}} - x_3 - a^{bq} kb \ln a (x_1 - x_4) \\ \dot{x}_2 &= c - dx_1^2 - x_2 \\ \dot{x}_3 &= r(s(x_1 - x_0) - x_3) \\ \dot{x}_4 &= x_5 - x_4^3 + b_1 x_4^2 + I_{\text{ext}} - x_6 - a^{bq} kb \ln a (x_4 - x_1) \\ \dot{x}_5 &= c - dx_4^2 - x_5 \end{aligned}$$

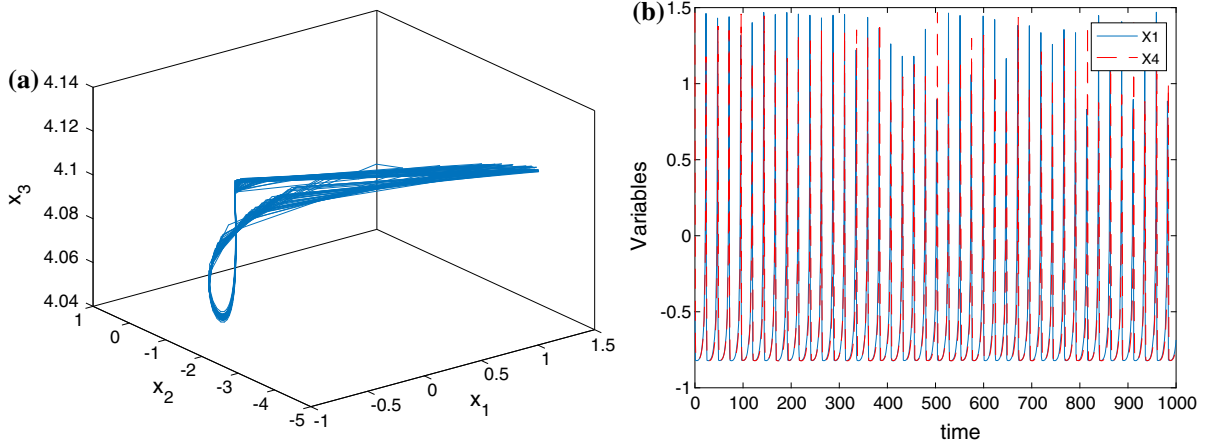


Fig. 17 **a** Three-dimensional x_1, x_2, x_3 plot shows dynamics of the system. **b** Time series plots of first variables x_1 and x_4 of neurons which are coupled through a memristor controlled by

$$\begin{aligned}\dot{x}_3 &= r(s(x_4 - x_0) - x_6) \\ \dot{u} &= x_1 - x_4\end{aligned}\quad (25)$$

The variable x_1 represents the membrane potential of a neuron, and the variables x_2 and x_3 are related ion currents across the membrane. The term $a^{bq}kb \ln a$ is a function that acts as exponential flux-controlled memristor. The parameters take values $a = e, b_1 = 3, c = 1, d = 5, r = 0.005, b = 50 \log(0.5), k = 10$. With the variation of external current, various dynamics are obtained as in Sect. 4.3.2.

4.3.1 Linear stability analysis

For exponentially flux-controlled memristor coupling with H–R neurons, the condition for stability is found to be

$$\tau < 2a^{bq}kb \ln a \quad (26)$$

For decremental flux-controlled memristor ($b < 0$) the condition for stability is reversed.

4.3.2 Phase portraits and time series plots of memristor coupled neurons controlled by exponential flux

Synchronization Phase portrait plots of second variables x_2 and x_5 of two H–R neurons coupled with exponential flux-controlled memristor show synchronization similar to that of H–R neurons coupled by quadratic flux-controlled memristor (Fig. 13).

exponential flux. When external current is set to $I_{\text{ext}} = 3$, tonic spike synchronization of neurons is obtained

Response to external current The response of membrane potential of two coupled neurons with respect to time is examined in detail which is shown in Fig. 17. When the external current is set to $I_{\text{ext}} = 3$, as the neuron is stimulated the membrane potential will change. Initially due to stimulating ionic currents, the membrane potential will increase. After a certain point, the inhibitory ionic currents will dominate the stimulating currents and the membrane potential will decrease which results in a spike which represents action potential. If this behaviour is persistent, then it is called tonic spiking.

Bursting synchronization As the external current is changed bursting synchronization is resulted and the corresponding phase space plot of two H–R neurons coupled with exponential flux-controlled memristor shows (Fig. 18) interesting dynamics.

Oscillation death Time series plots of first variables x_1 and x_4 of two H–R neurons coupled with exponential flux-controlled memristor show oscillation death for certain parameter values. If the parameter values a, b, d and I_{ext} are chosen as $a = 1, b = 0.01, d = 2.82$ and $I_{\text{ext}} = 3.8$, the two neurons approach a stable rest state as in the case of quadratic flux-controlled memristor as shown in Fig. 14.

4.3.3 Lyapunov exponent plot

Dynamics of Lyapunov exponent of H–R neurons coupled with exponential flux-controlled memristor are

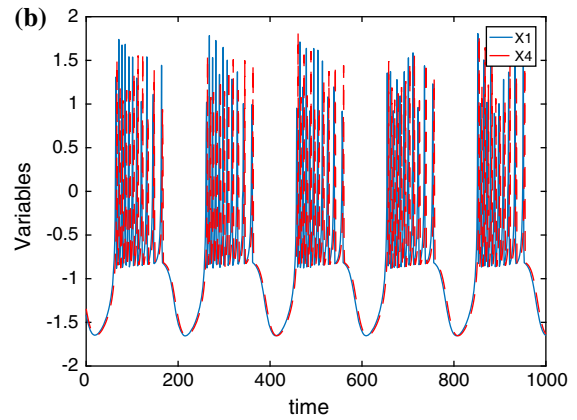
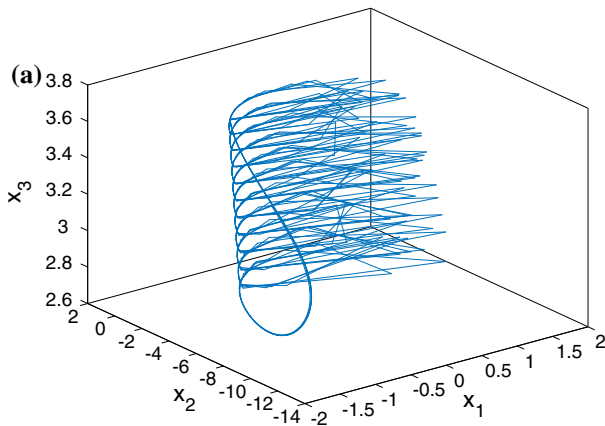
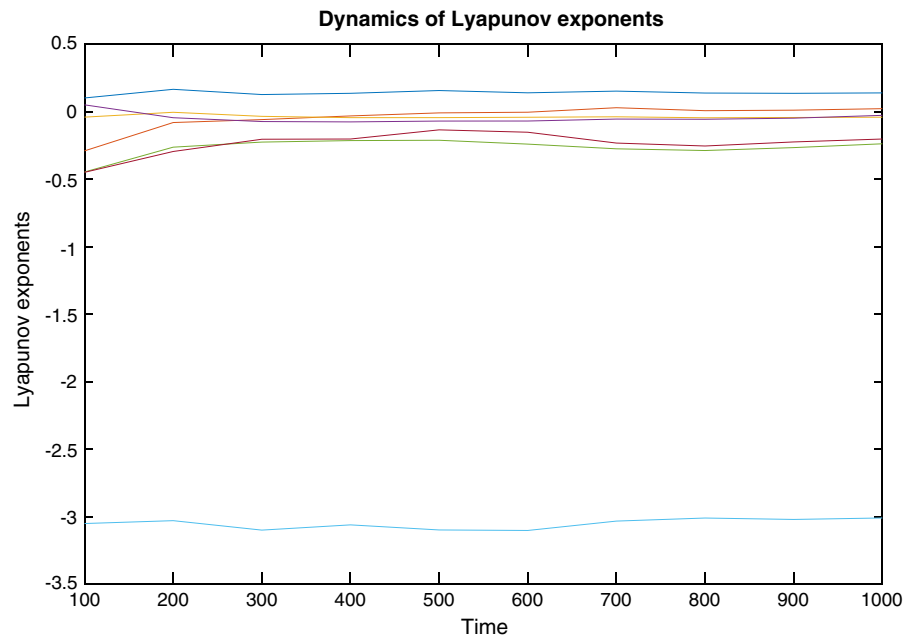


Fig. 18 **a** Dynamical behaviour of system shown through three-dimensional x_1, x_2, x_3 plot. **b** Time series plots of first variables x_1 and x_4 shows bursting synchronization of neurons where cou-

pling is due to memristor which is controlled by exponentially varying flux and here external current is set to $I_{ext} = 4$

Fig. 19 Lyapunov exponent plot for H–R neurons coupled with exponentially flux-controlled memristor



shown in Fig. 19. Higher value reflects greater sensitivity, and low values represents regularity.

Among different memristor coupling, cubic flux-controlled memristor coupling in H–R neurons shows more chaotic behaviour since it has largest Lyapunov value which is close to one (1).

5 Conclusion

The present work describes the possibilities of linear and nonlinear coupling in neurons. It has implications

for the analysis and characterization of neuronal interactions.

Linear models of effective connectivity in brain assume that the multiple inputs to a brain region are linearly separable. This assumption does not allow activity-dependent connections. This problem is overcome by adopting nonlinear models that include nonlinear interactions among inputs. These interactions can be considered as a context- or activity-dependent modulation of the influence that one region exerts over another [50].

The present work establishes the fact that indirect synaptic coupling dynamics of H–R neurons exhibits the properties like synchronization, anti-phase synchronization and amplitude death. As feedback coupling is varying in a cubic order, synchronization and anti-synchronization regions are observed.

In this study different memristor-based couplings are also taken into account. Both bidirectional and unidirectional couplings of cubic flux-controlled memristor in H–R neurons are examined. Mutual coupling of two neurons governed by H–R equations exhibits the properties of synchronization with tonic spiking and bursting. It also exhibits the property of amplitude death for certain values of coupling parameters. The unidirectional coupling shows tonic spiking or bursting for one of the neurons and death-like phenomenon for the uncoupled neuron depending upon the coupling coefficient and external current.

Memristor coupling of quadratic order shows the behaviour of synchronization, oscillation death and other interesting dynamics like near-death rare spikes for the neurons. Memristor controlled by exponential flux also showed the synchronization and oscillation death, but near-death rare spikes are found to be absent.

We have done the linear stability analysis for various couplings in H–R neurons. Lyapunov exponent plots are also examined in each case. It is observed that H–R neurons coupled with cubic flux-controlled memristor shows more chaotic nature.

The present work is on the effect of different coupling schemes in biological neuron model. The rich dynamical behaviour exhibited by the coupled systems depend upon system parameter values. We also intend to extend the work to latest developments in the field of memristor, such as spintronic memristor, and to its potential applications in neuromorphic circuits.

Acknowledgements We thank the referees for their constructive comments and suggestions. The authors would like to acknowledge the valuable suggestions from Mineeja K.K., Physics Department, St. Teresa's College, Ernakulam.

References

- Thornburg, K.S., Moller Jr., M., Roy, R., Carr, T.W., Li, R.D., Erneux, T.: Chaos and coherence in coupled lasers. *Phys. Rev. E* **55**, 38–3865 (1997)
- Kiss, I.Z., Gaspar, V., Hudson, J.L.: Experiments on synchronization and control of chaos on coupled electrochemical oscillators. *J. Phys. Chem. B* **104**(31), 7554–7560 (2000)
- Harrison, M.A., Lai, Y.C., Holt, R.D.: Dynamical mechanism for coexistence of dispersing species without trade-offs in spatially extended ecological systems. *Phys. Rev. E* **63**(051905), 519051–519055 (2001)
- Glass, L.: Synchronization and rhythmic processes in physiology. *Nature* **410**(6825), 277–284 (2001)
- Prasad, A., Dhamala, M., Adhikari, B.M., Ramaswamy, R.: Amplitude death in nonlinear oscillators with nonlinear coupling. *Phys. Rev. E* **81**, 027201 (2010)
- Koseska, A., Volkov, E., Kurths, J.: Oscillation quenching mechanisms: amplitude vs. oscillation death. *Phys. Rep.* **531**, 173–199 (2013)
- Ahn, S., Rubchinsky, L.L.: Short desynchronization episodes prevail in synchronous dynamics of human brain rhythms. *Chaos* **23**, 1–7 (2013)
- Arumugam, E.M.E., Spano, M.L.: A chimeric path to neuronal synchronization. *Chaos Interdiscip. J. nonlinear Sci.* **25**, 013107 (2015)
- Resmi, V., Ambika, G., Amritkar, R.E.: General mechanism for amplitude death in coupled systems. *Phys. Rev. E Stat. Nonlinear Soft Matter Phys.* **84**, 046212 (2011)
- Sharma, A., Sharma, P.R., Shrimali, M.D.: Amplitude death in nonlinear oscillators with indirect coupling. *Phys. Lett. Sect. A Gen. Atom. Solid State Phys.* **376**, 1562–1566 (2012)
- Saha, D.C.: On the synchronization of synaptically coupled nonlinear oscillators: theory and experiment. *Annu. Rev. Chaos Theory Bifurc. Dyn. Syst.* **6**, 1–29 (2016)
- Koch, A.J., et al.: Biological pattern formation: from basic mechanisms to complex structures. *Rev. Mod. Phys.* **66**, 1481–1507 (1994)
- Arbib, M.A.: *Handbook of Brain Theory and Neural Network*. MIT Press, Cambridge (2002)
- Zou, W., Senthilkumar, D.V., Nagao, R., Kiss, I.Z., Tang, Y., Koseska, A., Duan, J., Kurths, J.: Restoration of rhythmicity in diffusively coupled dynamical networks. *Nat. Commun.* **6**, 7709 (2015)
- Yu, H., Peng, J.: Chaotic synchronization and control in nonlinear-coupled Hindmarsh-Rose neural systems. *Chaos Solitons Fractals* **29**, 342–348 (2006)
- Volos, C.K., Kyprianidis, I.M., Stouboulos, I.N., Tlelo-Cuautle, E., Vaidyanathan, S.: Memristor: a new concept in synchronization of coupled neuromorphic circuits. *J. Eng. Sci. Technol. Rev.* **8**, 157–173 (2015)
- Matthews, P.C., Mirollo, R.E., Strogatz, S.H.: Complex time-delay systems: theory and applications. *Phys. D* **52** (1991)
- Prasad, A.: Time-varying interaction leads to amplitude death in coupled nonlinear oscillators. *Pramana J. Phys.* **81**, 407–415 (2013)
- Suresh, K., Sabarathinam, S., Thamilaran, K., Kurths, J., Dana, S.K.: A common lag scenario in quenching of oscillation in coupled oscillators. *Chaos Interdiscip. J. Nonlinear Sci.* **26**, 083104 (2016)
- Hens, C.R., Olusola, O.I., Pal, P., Dana, S.K.: Oscillation death in diffusively coupled oscillators by local repulsive link. *Phys. Rev. E Stat. Nonlinear Soft Matter Phys.* **88**, 034902 (2013)
- Wang, C., He, Y., Ma, J., Huang, L.: Parameters estimation, mixed synchronization, and antisynchronization in chaotic systems. *Complexity* **20**, 64–73 (2014)

22. Ma, J., Song, X., Jin, W., Wang, C.: Autapse-induced synchronization in a coupled neuronal network. *Chaos Solitons Fractals* **80**, 31–38 (2015)
23. Song, X., Wang, C., Ma, J., Tang, J.: Transition of electric activity of neurons induced by chemical and electric autapses. *Sci. China Technol. Sci.* **58**, 1007–1014 (2015)
24. Ma, J., Tang, J.: A review for dynamics of collective behaviours of network of neurons. *Sci. China Technol. Sci.* **58**, 2038–2045 (2015)
25. Ma, J., Qin, H., Song, X., Chu, R.: Pattern selection in neuronal network driven by electric autapses with diversity in time delays. *Int. J. Mod. Phys. B* **29**, 1450239 (2015)
26. Song, Y., Wen, S.: Synchronization control of stochastic memristor-based neural networks with mixed delays. *Neurocomputing* **156**, 121–128 (2015)
27. Berdan, R., Vasilaki, E., Khiat, A., Indiveri, G., Serb, A., Prodromakis, T.: Emulating short-term synaptic dynamics with memristive devices. *Sci. Rep.* **6**, 18639 (2016)
28. Merrih-Bayat, F., Bagheri-Shouraki, S.: Efficient neuro-fuzzy system and its memristor crossbar-based hardware implementation. **34** (2011). <https://arxiv.org/abs/1103.1156>
29. Wei, W., Min, Z.: Chaotic dynamics and its analysis of Hindmarsh-Rose neurons by Shil'nikov approach. *Chin. Phys. B* **24**(8), 1–6 (2015)
30. Hodgkin, A., Huxley, A.: A quantitative description of membrane current and its application to conduction and excitation in nerve. *J. Physiol. (Lond.)* **117**, 500–544 (1952)
31. Fitzhugh, R.: *Mathematical models for excitation and propagation in nerve*. Biological Engineering, vol. 5, pp. 1–85. Mc Graw (1969)
32. Morris, C., Lecar, H.: Voltage oscillations in the barnacle giant muscle fiber. *Biophys. J.* **35**(1), 193–213 (1981)
33. Hindmarsh, J.L., Rose, R.M.: A model of neuronal bursting using three coupled first order differential equations. *Proc. R. Soc. Lond. Biol.* **221**, 87–102 (1984)
34. Alias, L.A., Pai, M.S., George, M.M.V.: Near death experiences (NDE) of cardiac arrest survivors—a phenomenological study. *Mater. Methods* **3**, 216–220 (2015)
35. Zeren, T., Özbek, M., Kutlu, N., Akilli, M.: Significance of using a nonlinear analysis technique, the Lyapunov exponent, on the understanding of the dynamics of the cardiorespiratory system in rats. *Turk. J. Med. Sci.* **46**, 159–165 (2016)
36. Terman, D., Kopell, N., Bose, A.: Dynamics of two mutually coupled slow inhibitory neurons. *Phys. D Nonlinear Phenom.* **117**, 241–275 (1998)
37. Fang, X.: Chaotic synchronization of Hindmarsh–Rose neurons coupled by cubic nonlinear feedback. In: *Advances in Cognitive Neurodynamics ICCN 2007*, pp. 315–320 (2007)
38. Chua, L.: Memristive devices and systems. *Proc. IEEE* **64**(2), 209–223 (1976)
39. Mazumder, P.: Memristors: devices, models and application. *Proc. IEEE* **100**(6), 1911–1919 (2012)
40. Stockwell, R.: *English words: history and structure*. Cambridge Univ Press, Cambridge (2001)
41. Corinto, F.: Memristor synaptic dynamics' influence on synchronous behaviour of two Hindmarsh–Rose neurons. In: *2011 International Joint Conference on Neural Networks (IJCNN)*, pp. 2403–2408. IEEE (2011)
42. Johnson, R.C.: Missing link' memristor created. *EE Times*. 04 (2008)
43. Abdurahman, A., Jiang, H., Teng, Z.: Finite-time synchronization for memristor-based neural networks with time-varying delays. *Neural Netw.* **69**, 20–28 (2015)
44. Wang, H.T., Chen, Y.: Firing dynamics of an autaptic neuron. *Chin. Phys. B* **24**(12) (2015). doi:[10.1088/1674-1056/24/12/128709](https://doi.org/10.1088/1674-1056/24/12/128709)
45. Guo, Q.: Properties of quadratic flux-controlled and charge-controlled memristor. *Adv. Eng. Res.* 2352–5401 (2015). doi:[10.2991/ameii.15.2015.269](https://doi.org/10.2991/ameii.15.2015.269)
46. Lee, U., Borjigin, J.: Surge of neurophysiological coherence and connectivity in the dying brain. *PNAS* **110**(35), 144432–144437 (2013)
47. Klotz, I.: Brain waves surge moments before death. *Chin. Phys. B* **24**(8), 118401 (2009)
48. Yong, E.: In: *Dying brains, signs of heightened consciousness*. PNAS (2013)
49. Wei, L.: Exponential flux-controlled memristor model and its floating emulator. *Chin. Phys. B* **24**(11) (2015)
50. Friston, K.J.: Book review: brain function, nonlinear coupling, and neuronal transients. *Neuroscientist* **7**, 406–418 (2001)